Wave-Packet Dynamics in Nonlinear Disordered Chains under the Effect of Acoustic Waves

*Messias de Oliveira Sales, Adhemar Ranciaro Neto, and Francisco Anacleto Barros Fidelis de Moura**

In this work, the wave-packet dynamics is considered under the effect of diagonal disorder distribution, electron–lattice interaction, and acoustic-wave pumping. Electronic transport is taken into account quantum mechanically, whereas lattice vibrations are described through a classical nonlinear Morse Hamiltonian. The electronic hopping term takes the form of an exponential function of the effective distance between nearest-neighbor lattice elements. The electron wave-packet is initially localized at the first site of the chain alongside a Gaussian pulse generator. The results suggest that the disorder distribution breaks down the solitonic energy profile that exists within this kind of nonlinear Morse lattice. On the other hand, it is shown that the acoustic pumping sustains the wave packet dynamics within this disordered nonlinear model.

1. Introduction

The interaction between electronic wave packets and surface acoustic waves (SAW) in low-dimensional systems has attracted a substantial amount of interest, covering a wide range of subjects.[1–15] In ref. [3], a two-dimensional electron model in low temperatures was investigated on GaAs/Ga_{1-x}AlAs hetero-junctions under effect of strong magnetic fields and SAW. There it was observed that the interaction between SAW and the electron gas yields rich physics. Moreover, at high SAW intensities, a direct dependence of the electron conductivity upon the SAW propagation was shown. Further experimental studies on this subject were also carried out addressing, e.g., the electronic flux mediated by SAW in GaAs−AlGaAs heterostructures[5,6] and showing evidence of charge transport of electrons and holes at room temperature in an InGaAs/GaAs hetero-structure.[7] In a recent, interesting experiment reported in ref. [8], the authors managed to push an electronic wave-packet trough a wire. As a result, it was pointed out the possibility of using that kind of behavior to move, for example, a qubit between two distant places.[8] In summary, the electronic wave packet was trapped in a quantum dot and SAW were ultimately used to push the electron along the channel. In ref. [13], the authors demonstrated experimentally the possibility of manipulation of the charge carrier injection into self-assembled quantum dots (QD) and quantum posts (QP) by using SAW propagation, thereby paving the way for many applications within this context. Another interesting work was carried out in ref. [14], where SAW were applied in order to control carrier injection into a single InGaAs/GaAs quantum dot.

The interaction between electronic dynamics and lattice vibrations possess a key role in charge transport in low-dimensional systems. In ref. [16] the authors lattice deformations in Polyacetylene, including the energy of formation, length, mass, and activation energy for motion. They demonstrated that these lattice deformations play a fundamental role in the charge-transfer mechanism of Polyacetylene.[16] In the framework of electronic transport mediated by electron–lattice interaction, we must highlight Davydov's contribution.[17–24] He was one of the first scientists who proposed the idea that the electron–lattice nonlinear term promotes charge transport. Davydov's theory basically follows the assumption of a nonlinear interaction between a linear electronic model and a linear lattice dynamically described by a soliton-bearing equation. Other interesting works can be found in refs. [25–38]. M.G. Velarde and co-workers demonstrated the existence of a polaron-soliton "quasi-particle" in nonlinear lattices and also proposed the possibility of use this phenomenology in order to increase charge transport.

In this work we analyze the electronic propagation under the effect of nonlinearity, disorder and of an external acoustic wave. Nonlinearity is taken into account through the standard Morse–Toda interaction.[38] We emphasize that models featuring all those elements mentioned above are absent in the literature.[33,15] We define a quantum Hamiltonian to model electronic transport and a classical nonlinear Hamiltonian that accounts for the lattice vibrations. By assumption, the electron–lattice interaction varies exponentially with the effective distance between neighboring atoms. We obtain the dynamics which rises from an initial wave packet localized at the far left side of the chain and Gaussian pulse created at the same side. Our results show that the disorder

Dr. M. O. Sales
IFMA Campus São João dos Patos
rua Padre Santiago, s/n
Centro, São João dos Patos-MA, 65665-000, Brazil
Dr. A. R. Neto
Faculdade de Economia
Administração e Contabilidade
Universidade Federal de Alagoas
Maceió, AL 57072-970, Brazil
Dr. F. A. B. F. de Moura
Instituto de Física
Universidade Federal de Alagoas
Maceió, AL 57072-970, Brazil
E-mail: fidelis@fis.ufal.br

DOI: 10.1002/pssb.201800242

distribution destroys the solitonic energy profile that is expected in this class of nonlinear Morse lattice. Also, the acoustic wave pumping associated to the electron–lattice interaction generates wave-packet dynamics even at the presence of intense disorder.

2. Model

We consider a single electron moving in a 1*D* nonlinear lattice with *N* masses. The electronic Hamiltonian H_e can be defined as ref. [38]

$$H_e = \sum_n \epsilon_n Z_n^\dagger Z_n + \sum_n V_{n+1,n}\left(Z_{n+1}^\dagger Z_n\right) \tag{1}$$

where $Z_n^\dagger$ and Z_n are the creation and annihilation operators for the electron at site n, ϵ_n represents the on-site disorder distribution – uniformly chosen within the interval $[-W/2, W/2]$ –, and $V_{n+1,n}$ is the energy transfer between the nearest sites. The nonlinear lattice is primarily defined by taking into account the nearest-neighbor sites coupled by the Morse Potential. The classical Hamiltonian H_{lattice} is given by

$$H_{\text{lattice}} = \sum_n \frac{p_n^2}{2M_n} + Y_1\left\{1 - \exp\left[-Y_2\left(q_n - q_{n-1}\right)\right]\right\}^2 \tag{2}$$

where p_n and q_n are the momentum and displacement of the mass at site (n), respectively. Y_1 is typical bond energy and Y_2 is the range parameter of the Morse potential.[38] We consider M_n to follow disorder distribution generated upon the following procedure: $M_n = e^{(\Pi_n)}$, with Π_n, are random numbers uniformly distributed within the interval $[-W/2, W/2]$. Constants Y_1 and Y_2 were defined as in ref. [38]: $q_n \to Y_2 q_n$, $p_n \to p_n/\sqrt{2Y_1}$, and $H_{\text{lattice}} \to H_{\text{lattice}}/(2Y_1)$.

The electron–lattice interaction in the model above depends on the coefficients of electronic states and displacements of molecular masses from their equilibrium positions. The hopping elements $V_{n+1,n}$ are functions of the relative distance between two consecutive molecules in the chain following $V_{n+1,n} = -V\,\exp\left[-a\left(q_{n+1} - q_n\right)\right]$. The parameter a represents the degree of relative displacement of the lattice in units of the hopping term, $V_{n+1,n}$. In other words, it determines the electron-lattice coupling strength (in units of $1/Y_2$). For a small relative displacement we recover the Su-Schrieffer-Heeger approximation, $V_{n+1,n} \approx -V\left[1 - a\left(q_{n+1} - q_n\right)\right]$.[16] We would like emphasize that the Morse nonlinearity consider at this present work is quite distinct from the harmonic description addressed in ref. [15]. The Morse potential promotes the appearance of solitonic modes within the lattice and also stands out as one the most convenient ways to model the vibrational profile for a wide range of molecules.[33]

The time-dependent wave function $|\Phi(t)\rangle = \sum_n c_n(t)|n\rangle$ is obtained by numerical evaluation of the time-dependent Schrödinger equation. The Wannier amplitudes evolve in time according to the time-dependent Schrödinger equation ($\hbar = 1$)

$$i\frac{dc_n(t)}{dt} = \epsilon_n c_n(t) - \tau\exp\left[-a\left(q_{n+1} - q_n\right)\right]c_{n+1}(t) - \tau\exp\left[-a\left(q_n - q_{n-1}\right)\right]c_{n-1}(t) \tag{3}$$

The lattice equation is written as

$$\begin{aligned} M_n\frac{d^2q_n(t)}{dt^2} = {} & \left\{\left\{1 - \exp\left[-\left(q_{n+1} - q_n\right)\right]\right\}\exp\left[-\left(q_{n+1} - q_n\right)\right]\right. \\ & -\left\{1 - \exp\left[-\left(q_n - q_{n-1}\right)\right]\right\}\exp\left[-\left(q_n - q_{n-1}\right)\right] \\ & +aV\left\{\left(c_{n+1}^* c_n + c_{n+1}c_n^*\right)\exp\left[-a\left(q_{n+1} - q_n\right)\right]\right. \\ & \left.\left.-\left(c_n^* c_{n-1} + c_n c_{n-1}^*\right)\exp\left[-a\left(q_n - q_{n-1}\right)\right]\right\}\right\} \end{aligned} \tag{4}$$

Here, time is rescaled as $t \to \Omega t$, where Ω is the frequency of harmonic oscillations around the minimum of the Morse potential.[38] The generalized quantity $\tau = V/(\hbar\Omega)$ thus determines the timescale difference between the (fast) electronic dynamics and (slow) lattice vibrations. Following the ref. [38] we consider $V = 0.1$ and $\tau = 10$.

When $t = 0$ we set the electron on site $n = 1$, i.e., $|\Phi(t=0)\rangle = \sum_n c_n(t=0)|n\rangle$, where $c_n(t=0) = \delta_{n,1}$. We further consider $q_n(t=0) = \dot{q}_n(t=0) = 0$ for n within the interval [1, *N*]. Moreover, we put an acoustic Gaussian pulse generator at the far left side of chain (i.e., at the site $n = 0$):

$$q_0(t) = A_0 e^{\left(-t^2/2\Delta t^2\right)}\cos(\omega t) \tag{5}$$

where ω is the frequency of the Gaussian acoustic pulse and $\Delta t = 1/\Delta\omega$ is the time width. Our analysis is done through numerical solutions of the Equations (3) and (4). In particular, the electronic propagation is obtained by employing a high-order Taylor expansion of the time evolution operator $U(\delta t)$[41] of the form

$$U(\delta t) = \exp\left(-i\tilde{H}_e\delta t\right) = 1 + \sum_{l=1}^{n_o}\frac{\left(-i\tilde{H}_e\delta t\right)^l}{l!} \tag{6}$$

where $\tilde{H}_e$ is exactly the same one-electron Hamiltonian (1) with normalized hopping $\tilde{V}_{n+1,n} = -\tau\exp\left[-a\left(q_{n+1} - q_n\right)\right]$. The wave-function at time δt is given by $|\Phi(\delta t)\rangle = U(\delta t)|\Phi(t=0)\rangle$. This method may be used recursively to get the wave-function at time t (for details, see ref. [39]). The classical equations (4) are solved with a high-order Euler method.[40] It starts with a standard Euler method so as to find an initial prediction $q_n^0(\delta t)$ at time δt: $q_n^0(\delta t) \approx q_n(t=0) + \delta t\frac{dq_n}{dt}|_{t=0}$. Atomic vibrations at time $\delta t\left(q_n(\delta t)\right)$ are then obtained by the recursive formula:

$$q_n(\delta t) \approx q_n^{l_0}(\delta t) \approx q_n(t=0) + \frac{\delta t}{2}\left[\left.\frac{dq_n}{dt}\right|_{t=0} + \left.\frac{dq_n^{l_0-1}}{dt}\right|_{\delta t}\right] \tag{7}$$

where l_0 denotes the number of steps. Our results were obtained with $\delta t = 5\times10^{-3}$, $n_o = 12$, and $l_0 = 4$. We stress that we compared our results with data obtained from standard methods (fourth-order Runge-Kutta (RK4),[40] for example, which lasts twice as longer) and did not find any relevant qualitative difference between them. In order to proceed with the electronic transport analysis we computed the electronic mean position

(centroid) defined as $\langle n(t)\rangle = \sum_n (n)|c_n(t)|^2$ and the Shannon entropy $S(t) = -\sum_n |c_n(t)|^2 \ln|c_n(t)|^2$.[41,42] The centroid in a given time t represents the mean position of the electron using the center of a self-expanded chain as the origin. The entropy $S(t)$ goes from 0, when the wave function is confined to a single site, to $\log(N)$ when it gets uniformly extended over the whole chain. The Shannon entropy thus estimates the size of the wave packet at time t.

3. Results

Numerical data were obtained for a very long chain featuring $N > 10^4$ sites. However, we started the procedure with a small chain with N^* sites located at the left side (i.e., the differential equations were initially solved within the region $[1, N^*]$). Whenever the sum $B = \left(|c_{N^*}(t)|^2 + |q_{N^*}(t)|\right)$ exceeded 10^{-20}, ten new sites were added to N^*. This trick (called "self expanded chain") is an useful tool to avoid unwanted boundary effects. We set $N^* = 300$ sites. For long times ($\approx 2 \times 10^4$ time units) N^* became larger than 10^4. According to Anderson localization theory, any amount of uncorrelated disorder ($W > 0$) promotes the degradation of electron propagation for an one-dimensional lattice. Here we have considered $W \geq 1$ given it is not very convenient to work at the weak disorder limit ($W \ll 1$) from a numerical point of view.

In **Figure 1** we depict the overall electronic dynamics of our model. Also, we plot the electronic mean position $\langle n(t)\rangle$(A − C) and the Shannon entropy $S(t)$ (E–F) versus time for various ω and a values. For $a = 0$ both quantities remained constant at the long-time limit. It comprises a clear signature of the standard Anderson's localization phenomenology. As the electron–lattice interaction ($a > 0$) is increased, both the centroid ($\langle n(t)\rangle$) and the Shannon Entropy ($S(t)$) exhibited a sub-diffusive dynamics. This behavior is a clear breakdown of the Anderson's localization. Formally, for $a > 0$, we have here a one-dimensional disordered nonlinear system which allows for electronic propagation. The electron–lattice coupling promotes an effective link between the electron and the acoustic wave that propagates along the chain. Therefore, the electron is carried along the disordered nonlinear chain by the lattice's deformations. In **Figure 2**, we analyzed the wave function profile along time (i.e., $|c_n((t)|^2 \times t \times n$). Calculations were done for fixed $W = 1.0$, $\omega = 0.02$, and several a values. We stress that the wave packet was initially prepared at the site $n = 1$ (i.e., the left side of the chain). While tracking down the wave packet evolution through the time, we observed that, for $a > 0$, it splits itself into two parts: a fast solitonic mode and a slower wave packet that remains close to the left side ($n = 1$) of the chain. This is due to the presence of the Morse potential in our model. We emphasize that when an initial amount of energy is injected in a nonlinear Morse chain, a finite fraction of this initial energy propagates along the chain in a solitonic-like profile; the other part evolves along the chain

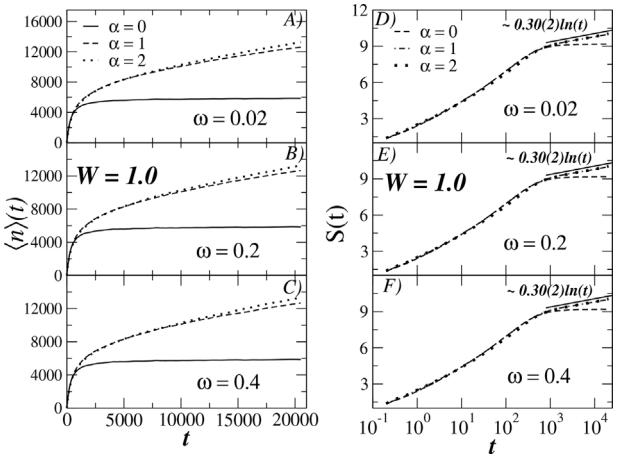

Figure 1. Electronic mean position $\langle n(t)\rangle$ (A–C) and Shannon entropy $S(t)$ (D–F) versus time for $\omega = 0.02$, 0.2, and 0.4; $W = 1$; and $\alpha = 0.0$, 1.0, and 2.0. For $\alpha > 0$ we found a clear signature of the breakdown of Anderson localization. Due to the effective coupling with the acoustic pumping, the centroid ($\langle n(t)\rangle$) and the Shannon Entropy ($S(t)$) both exhibit sub-diffusive dynamics.

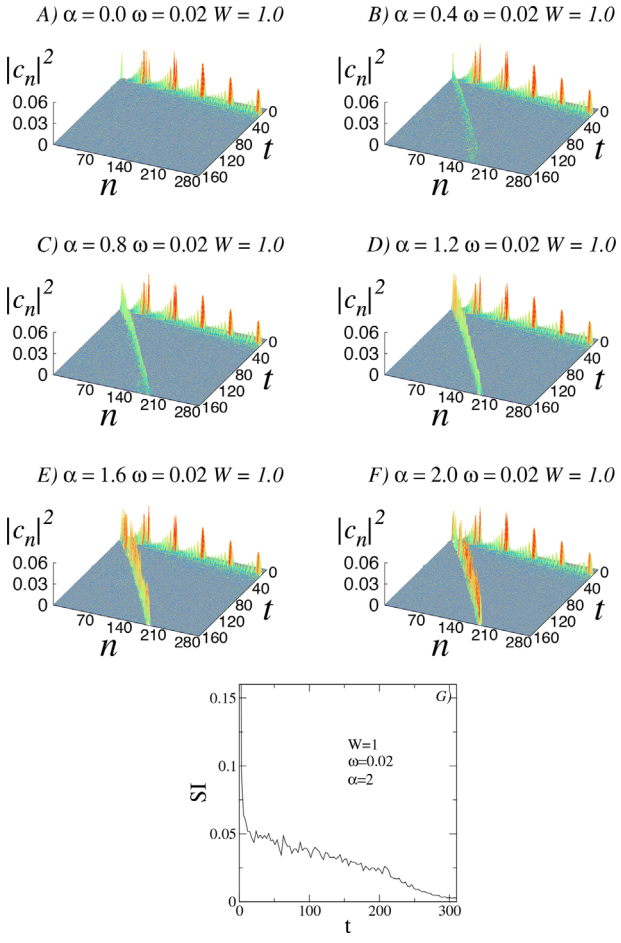

Figure 2. A–F) Square modulus of the electronic wave-packet ($|c_n((t)|^2$) versus t and n for $W = 1.0$, $\omega = 0.02$ and $\alpha = 0.0$, 0.4, 0.8, 1.2, 1.6, and 2.0. For $\alpha > 0$ the initially localized wave packet splits into two: a solitonic-like mode (cf. pronounced peaks along the diagonal of the plane $n \times t$) and a free component close to the initial site. G) Soliton intensity (SI) versus time t for $W = 1$, $\alpha = 2$, and $\omega = 0.02$. For long times, disorder destroys the solitonic propagation.

through nonlinear vibrational modes, often called radiation (see refs. [43,44]). This phenomenon occurs in one-dimensional chains even in the absence of disorder ($W = 0$). As disorder is increased in low-dimensional systems (1d in particular), the solitonic and radiation components are still present for short times. For long times, however, they get damped by Anderson Localization.

A brief summary of the vibrational energy propagation is given in **Figure 3**A and B. We ploted the lattice deformation $A_n = |e^{q_n - q_{n-1}} - 1|$ versus n and t for $W = 1.0$, $\omega = 0.02$, (A) $\alpha = 0.4$e (B) 2.0. When analyzing these results, we noticed the existence of two key aspects within the lattice deformation: a solitonic-like deformation (close to the diagonal of ntimest plane) and a strong diffusive radiation (see the region between the diagonal of plane $n \times t$ and line $n = 1$). Therefore, these two kinds of nonlinear vibrations, which exist within the disordered Morse chain (solitonic like mode and radiation), capture two distinct portions of the initial electronic wave-packet due to the electron–lattice coupling. It explains the two branches of electronic wave packet profile in Figure 2. In addition to that, there is intrinsic compositional disorder (with strength W) which scatters both the solitonic mode and the portion of wave-packet that propagates separately close to the left side. Therefore, due the presence of disorder, the intensity the of the solitonic like mode fades with time. In fact, by looking at Figure 2, we can see this behavior clearly for $0 < \alpha < 1$ (i.e., Figure 2B and C).

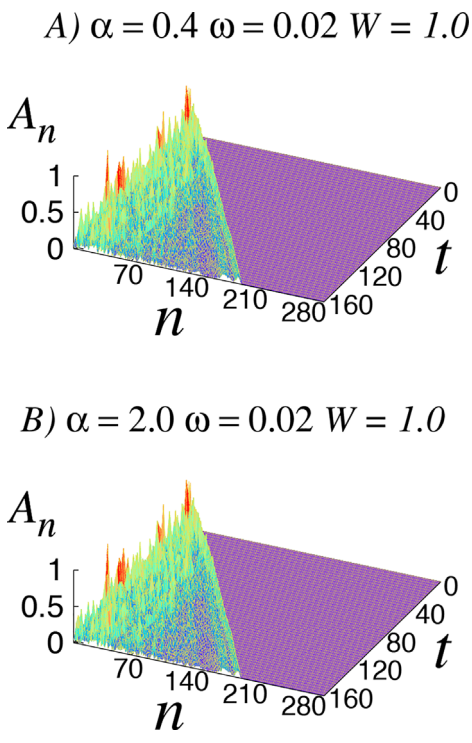

Figure 3. $A_n = |e^{q_n - q_{n-1}} - 1|$ versus n and t for $W = 1.0$, $\omega = 0.02$ and A) $\alpha = 0.4$, B) $\alpha = 2.0$. Pumping an acoustic mode at the left side of the chain promotes the appearance of two kinds of lattice vibrations: a solitonic-like propagation (located closely to the diagonal of plane $n \times t$) and a strong and diffuse radiation located between the diagonal of plane $n \times t$ and the line $n = 1$.

However, for $\alpha > 1$ that is not so clear (see Figure 2D–F) . To better explore the solitonic dynamics for large α, we show the soliton intensity ($SI = |c_s(t)|^2$) versus time t in Figure 2G for $W = 1$, $\alpha = 2$ and $\omega = 0.02$. We emphasize that $SI = |c_s(t)|^2$, where s represents the position of the solitonic like mode along time. The fading of the solitonic mode for long times is now more evident, what brings us to state that the solitonic behavior holds only for short timescales. Note that the electronic wave packet still spreads in the long-time regime.

In **Figure 4**A–F, we investigated the dependence of our results upon disorder strength W and pumping frequency ω. In Figure 4A–D we plot the centroid $\langle n(t) \rangle$ and the Shannon Entropy $S(t)$ versus time. There we see that even for intense disorder sub-diffusive dynamics is obtained. This clearly represents a strong violation of Anderson localization. Our data demonstrated that the coupling between the electron and acoustic pumping promotes electronic propagation within a nonlinear system even at the intense disorder limit. In Figure 4E and F we plot the long-time value of the centroid $\langle n(t \approx 2 \times 10^4) \rangle$ and the Shannon entropy $S(t \approx 2 \times 10^4)$ versus ω. We observe that until $\omega \approx 2$, the electronic wave

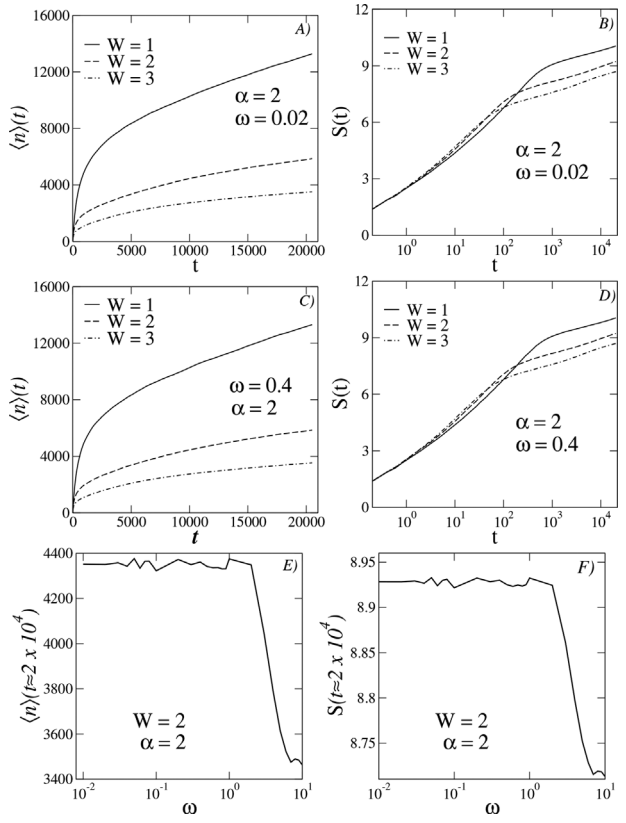

Figure 4. A–D) Centroid $\langle n(t) \rangle$ and Shannon entropy $S(t)$ versus time for $\omega = 0.02$, 0.4, $\alpha = 2$, and $W = 1$, 2, 3. Our calculations indicate that the sub-diffusive dynamics is obtained even for strong disorder (i.e., $W > \langle V_{n,n+1} \rangle$)). E, F) Long-time profile of the centroid $\langle n(t \approx 2) \times 10^4 \rangle$ and Shannon entropy $S(t \approx 2 \times 10^4)$ versus ω. From $\omega = 0.02$ to $\omega \approx 2$, the electronic wave packet keeps its velocity and width approximately constants. For $\omega > 2$ the velocity and the width of the wave packet exhibited slightly decreasing values.

packet keeps its velocity and width approximately constants. For $\omega > 2$ the electronic velocity and the width of the wave packet decreases a little bit. We point out that the Shannon Entropy seems to be less dependent upon the pumping frequency ω. We argue that is due to the logarithmic behavior of $S(t)$. Small modifications on the shape of the electronic wave packet promote about negligible changes on the long-time behavior of $S(t)$. In disordered harmonic chains, high frequencies also exhibit slower propagation. In general, acoustic modes with high frequency have small wavelength and, according to standard Anderson localization theory, modes with small wavelengths are scattered by the disorder more easily. We believe that within this nonlinear disordered chain a similar phenomenology occured.

4. Conclusions

In this work we have investigated the dynamics of a single electron in a Morse chain subjected to disorder and in the presence of an external acoustic wave. We have used a quantum mechanics formalism to describe the electron transport and a classical nonlinear Hamiltonian for the lattice vibrations. We emphasize that our model contains two distinct sources of disorder: disorder within the on-site energies and at the mass distribution. Therefore, both dynamics quantum and classical equations contains disordered terms. The electron–lattice interaction was incorporated into the model through a hopping term defined as an exponential function of the effective distance between the nearest neighbors masses. By initializing the system with a fully localized wave packet at the left end of the chain and placing a Gaussian acoustic pulse generator at the same side, we observed that the acoustic wave associated with the electron–lattice interaction is able to sustain the wave packets dynamics even at the presence of intrinsic disorder. We also investigated the dependence of the electronic transport upon frequency of the Gaussian pulse, ω. In summary, for large ω the electronic propagation became slightly slower.

Acknowledgements

The research was partially supported by the Brazilian research agencies CNPq, CAPES, INCT-Nano(Bio)Simes, as well as FAPEAL (Alagoas State Agency). We are grateful to G. M. A. Almeida for useful discussions, corrections, and suggestions.

Conflict of Interest

The authors declare no conflict of interest.

Keywords

electron–phonon coupling, nonlinear lattices, sub-diffusive spreading, wave packet dynamics

Received: May 29, 2018
Revised: August 15, 2018
Published online:

[1] C. J. B. Ford, *Physica Status Solidi B* **2017**, *254*, 1600658.
[2] C. Bödefeld, A. Wixforth, J. Toivonen, M. Sopanen, H. Lipsanen, *Physica Status Solidi B* **2001**, *224*, 703.
[3] A. Wixforth, J. P. Kotthaus, G. Weimann, *Phys. Rev. Lett.* **1986**, *56*, 2104.
[4] M. Rotter, A. V. Kalameitsev, A. O. Govorov, W. Ruile, A. Wixforth, *Phys. Rev. Lett.* **1999**, *82*, 2171.
[5] J. M. Shilton, D. R. Mace, V. I. Talyanskii, Y. Galperin, M. Y. Simmons, M. Pepper, D. A. Ritchie, *J. Phys.: Condens. Matter* **1996**, *8*, L337L343.
[6] J. M. Shilton, V. I. Talyanskii, M. Pepper, D. A. Ritchie, J. E. F. Frost, C. J. B. Ford, C. G. Smith, G. A. C. Jones, *J. Phys.: Condens. Matter* **1996**, *8*, L531.
[7] M. Streibl, A. Wixforth, J. P. Kotthaus, A. O. Govorov, C. Kadow, A. C. Gossard, *Appl. Phys. Lett.* **1999**, *75*, 4139.
[8] R. P. G. McNeil, M. Kataoka, C. J. B. Ford, C. H. W. Barnes, D. Anderson, G. A. C. Jones, I. Farrer, D. A. Ritchie, *Nature* **2011**, *477*, 439.
[9] C. H. W. Barnes, J. M. Shilton, A. M. Robinson, *Phys. Rev. B* **2000**, *62*, 8410.
[10] M. R. Astley, M. Kataoka, C. J. B. Ford, C. H. W. Barnes, D. Anderson, G. A. C. Jones, I. Farrer, D. A. Ritchie, M. Pepper, *Phys. Rev. Lett.* **2007**, *99*, 156802.
[11] H. Sanada, T. Sogawa, H. Gotoh, K. Onomitsu, M. Kohda, J. Nitta, P. V. Santos, *Phys. Rev. Lett.* **2011**, *106*, 216602.
[12] M. R. Astley, M. Kataoka, C. J. B. Ford, C. H. W. Barnes, D. Anderson, G. A. C. Jones, I. Farrer, D. A. Ritchie, M. Pepper, *Physica E* **2008**, *40*, 1136.
[13] S. Volk, F. J. R. Schülein, F. Knall, D. Reuter, A. D. Wieck, T. A. Truong, H. Kim, P. M. Petroff, A. Wixforth, H. J. Krenner, *Nano Lett.* **2010**, *10*, 33993407.
[14] F. J. R. Schülein, K. Müller, M. Bichler, G. Koblmüller, J. J. Finley, A. Wixforth, H. J. Krenner, *Phys. Rev. B* **2013**, *88*, 085307.
[15] A. Ranciaro Neto, M. O. Sales, F. A. B. F. de Moura, *Solid State Commun.* **2016**, *229*, 2227.
[16] W. P. Su, J. R. Schrieffer, A. J. Heeger, *Phys. Rev. Lett.* **1979**, *42*, 1698.
[17] A. S. Davydov, *Solitons in Molecular Systems*, 2nd ed., Reidel, Dordrecht **1991**.
[18] A. C. Scott, *Phys. Rep.* **1992**, *217*, 1.
[19] A . S. Davydov, *Phys. Scr.* **1979**, *20*, 387.
[20] A. S. Davydov, *J. Theor. Biol.* **1977**, *66*, 379.
[21] A. S Davydov, *Biology and Quantum Mechanics*. Pergamon, New York **1982**.
[22] A. S. Davydov, N. I. Kislukha, *Phys. Status Solidi B* **1976**, *75*, 1.
[23] A. S. Davydov, *Phys. Status Solidi B* **1978**, *90*, 457.
[24] A. S. Davydov, *Phys. Status Solidi B* **1986**, *138*, 559.
[25] B. J. Alder, K. J. Runge, R. T. Scalettar, *Phys. Rev. Lett.* **1997**, *79*, 3022.
[26] L. S. Brizhik, A. A. Eremko, *Physica D* **1995**, *81*, 295.
[27] O. G. Cantu Ross, L. Cruzeiro, M. G. Velarde, W. Ebeling, *Eur. Phys. J. B* **2011**, *80*, 545.
[28] M. G. Velarde, C. Neissner, *Int. J. Bifurcation Chaos* **2008**, *18*, 885.
[29] M. G. Velarde, W. Ebeling, A. P. Chetverikov, *Int. J. Bifurcation Chaos* **2011**, *21*, 1595.
[30] A. P. Chetverikov, W. Ebeling, M. G. Velarde, *Eur. Phys. J. B* **2011**, *80*, 137.
[31] D. Hennig, M. G. Velarde, W. Ebeling, A. Chetverikov, *Phys. Rev. E* **2007**, *78*, 066606.
[32] M. G. Velarde, W. Ebeling, A. P. Chetverikov, *Int. J. Bifurcation Chaos* **2005**, *15*, 245.
[33] M. G. Velarde, *J. Comput. Appl. Math.* **2010**, *233*, 1432.
[34] M. G. Velarde, W. Ebeling, A. P. Chetverikov, *Eur. Phys. J. B* **2012**, *85*, 291.
[35] W. Ebeling, A. P. Chetverikov, G. Röpke, M. G. Velarde, *Contrib. Plasma Phys.* **2013**, *53*, 736.

[36] A. P. Chetverikov, W. Ebeling, M. G. Velarde, *Eur. Phys. J.—Spec. Top.* **2013**, *222*, 2531.
[37] M. G. Velarde, A. P. Chetverikov, W. Ebeling, E. G. Wilson, K. J. Donovan, *EPL* **2014**, *168*, 27004.
[38] D. Hennig, A. Chetverikov, M. G. Velarde, W. Ebeling, *Phys. Rev. E* **2007**, *76*, 046602.
[39] F. A. B. F. de Moura, *Int. J. M. Phys. C* **2011**, *22*, 63.
[40] E. Hairer, S. P. Norsett, G. Wanner, in *Numerical Recipes: The Art of Scientific Computing*, 3rd ed. (Eds: W. H. Press, B. P. Flannery, S. A. Teukolsky, W. T. Wetterling), Cambridge University Press, New York **2007**.
[41] M. O. Sales, F. A. B. F. de Moura, *J. Phys.: Condens. Matter* **2014**, *26*, 415401.
[42] F. A. B. F. de Moura, B. Santos, L. P. Viana, M. L. Lyra, F. A. B. F. de Moura, *Solid State Commun*. **2006**, *138*, 585.
[43] J. L. L. dos Santos, M. O. Sales, A. Ranciaro Neto, F. A. B. F. de Moura, *Phys. Rev. E* **2017**, *95*, 052217.
[44] N. F. Smyth, A. L. Worthy, *Phys. Rev. E* **1999**, *60*, 2330.